Electronic Supplementary Material (ESI) for Soft Matter.
This journal is © The Royal Society of Chemistry 2020

Probing particle heteroaggregation using analytical centrifugation

Marcel Rey[a,b], Maximilian J. Uttinger[a,b], Wolfgang Peukert[a,b],

Johannes Walter[a,b,] Nicolas Vogel[a,b,*]*

Corresponding authors: *johannes.walter@fau.de, *nicolas.vogel@fau.de

[a] Institute of Particle Technology (LFG), Friedrich-Alexander Universität Erlangen-Nürnberg (FAU), Cauerstrasse 4, 91058 Erlangen, Germany

[b] Interdisciplinary Center for Functional Particle Systems (FPS), Friedrich-Alexander Universität Erlangen-Nürnberg (FAU), Haberstrasse 9a, 91058 Erlangen, Germany

Experimental:

Materials:

All chemicals were purchased from commercial sources. N,N'-Methylenebis(acrylamide) (BIS; 99 %, Sigma Aldrich), ammonium persulfate (APS, Sigma Aldrich, 98 %), ethanol (EtOH, Sigma Aldrich, 99.9 %), potassium chloride (≥99.0%, Sigma Aldrich), hexane (≥ 99 %, Sigma Aldrich), sodium dodecyl sulfate (SDS, Sigma Aldrich, 98 %) were used as received.

N-Isopropylacrylamide (NIPAM; 97 %, Sigma Aldrich) was purified by recrystallization from hexane (95 %, Sigma Aldrich). Water was double deionized using a Milli-Q system (18.2 MΩ·cm, Elga™ PURELAB™ Flex).

Microgel synthesis: The set of PNIPAM microgels with similar size in the collapsed state but different crosslinking densities was synthesized by surfactant-free precipitation polymerization as described in a previous publication.[1] In short, in a 500 mL three-neck round bottom flask equipped with reflux condenser and stirrer, 2.83 g of NIPAM and 38.5 – 385 mg BIS were dissolved in 249 mL of water. The solution was heated to 80 °C and purged with nitrogen gas. After an equilibration for 30 minutes, the reaction was initiated by adding a solution of 14.3 mg of APS dissolved in 1 mL of water. After 5 hours of reaction, the suspension was cooled down to room temperature and purified by centrifugation and redispersion in water three times, followed by dialysis against water for one week and replacement of the water phase once per day.

Smaller PNIPAM microgels were synthesized using SDS as surfactant to control the size during the precipitation polymerization adapted by Wu et al..[2] In a 500 mL round-bottom flask equipped with condenser 3.4 g NIPAM, 0.23 BIS and 0.02 g SDS were dissolved in 195 mL water. The mixture was heated to 70 °C and degassed by bubbling nitrogen for 30 minutes. 0.1 g APS, dissolved in 5 mL water, was added to initiate the polymerization. The reaction was stopped after 4 hours. After cooling to room temperature, the dispersion was purified by centrifugation and redispersion as well as by dialysis against water for 2 months, changing the water each day to ensure removal of SDS.

Silica synthesis: The silica nanoparticles were synthesized *via* the Stöber process.[3] In short, to a mixture of 15 g TEOS (98 %, Sigma Aldrich) dissolved in 148 g ethanol (≥98.8 %, Sigma Aldrich), a mixture of 76 g ultrapure water, 48 g ethanol and 27 g ammonium hydroxide solution (30 %, Sigma

Aldrich) was added at room temperature under continuous stirring. The reaction mixture was stirred at 500 rpm for 16 hours. The particles were cleaned by centrifugation and redispersion for three times in ethanol and then three times in water respectively.

Dynamic light scattering and zeta potential: Dynamic light scattering experiments were performed with a Malvern Zetasizer Nano-ZS in disposable polystyrene cuvettes at a scattering angle of 173°. The diffusion coefficient and hydrodynamic diameter of the particles were measured as a function of the temperature, ranging from 20 to 50 °C. At each temperature step, the suspension was equilibrated for 15 minutes. The measurements were performed four times after equilibration for 180 s at each temperature. Similarly, the zeta potential was measured at 20 °C and at 40 °C using a NaCl concentration of 1 mM.

Partial specific volume measurement: Densities of dispersions with varying microgel concentrations were measured at 20 °C with an Anton Paar DMA 5000 M. The partial specific volume was calculated using the Kratky method and the density increment was determined according to Equation S1 at constant chemical potential μ.

$$\bar{\nu} = \frac{1 - \left(\frac{\partial \rho_{solution}}{\partial c}\right)_{\mu}}{\rho_s} \tag{S1}$$

For determination of the microgel concentrations, the microgel samples were dried in an oven (VWR, DRY-Line) and the powder was weighted using a fine balance (Satorius, M-Pact) prior to preparing the dispersions.

Analytical ultracentrifugation: Sedimentation velocity experiments for the determination of sedimentation coefficients were performed using a modified preparative centrifuge, type Optima L-90 K, from Beckman Coulter.[4] The temperature was set to 20 °C and 40 °C and equilibrated for at least 1 h at constant temperature. Titanium centerpieces with a path length of 12 mm were used for all experiments. The microgel dispersions were diluted to a defined adsorption of 0.8 at 300 nm measured by UV-VIS spectroscopy (Lambda 950 UV-VIS, PerkinElmer). Rotor speeds of 6000 rpm and 3000 rpm were used for the microgels in swollen and collapsed state, respectively. Sedimentation velocity data was analyzed using the ls-g*(s) method implemented in SEDFIT which provided the apparent

sedimentation coefficient distribution.[5] Diffusional broadening of the sedimentation boundaries could be safely neglected due to the large size of the microgels.

Electron microscopy: The heteroaggregates were further visualized by Scanning Electron Microscope (SEM) imaging using a Gemini SEM 500 from Zeiss using a 30 µm aperture, a voltage of 1 kV and the in-lens detector. After one day, the dispersion was diluted with water by 1:100 to avoid the adsorption of free microgels onto the silica particles during drying.[6]

Microgel characterisation using AUC:

An open question in the field of PNIPAM microgels is the density of the PNIPAM polymer. The first value reported by Lele et al. on the PNIPAM density was 1.26 g cm^{-3}.[7] However, the value needs to be treated with care as it is based on a fitting parameter assumed in a model explaining the experimental swelling behaviour of macroscopic PNIPAM gels.[7,8] Furthermore, the PNIPAM density has been measured by various experimental methods,[9,10] which we elaborate below. When comparing the results from those methods, attention has to be paid to the nature of the density that is measured.

By measuring the sedimentation and diffusion coefficient, the mass of the analyte can be calculated. Which kind of mass is derived by the AUC experiments depends on the input for the partial specific volume or inverse density. While the effective density including solvation will provide the total mass of the particle including solvent, the partial specific volume will give the anhydrous molar mass of the particle.[11] The partial specific volume is defined as the change in volume when adding particles of certain mass to the solution and can be experimentally determined when measuring the density of solutions with different analyte concentration, also referred to as Kratky's method.[12] It has to be noted that the mass of the dried and thus water-free microgel is required for the determination of the concentration. Any contributions of water will directly translate to the measured partial specific volumes and thus also the analyte masses derived by AUC.

Gradient experiments provide the anhydrous or effective density of the particle, depending on whether the density gradient forming solutes interact with the analyte and its solvation layer or not. Separate measurements in different solvents will lead to the partial specific volume analogous to Kratky's method as long as preferential adsorption does not occur. Assuming that the density of the solvation layer is identical to the bulk solvent density, the partial specific volume would resemble the inverse of the anhydrous density.

In a sucrose density gradient experiment, a PNIPAM density of 1.04 - 1.07 g cm^{-3} was measured.[10] Another group measured the density of PNIPAM microgels by AUC runs in two solvents with different densities.[9] Using H_2O/D_2O as solvents they measured a density of 1.19 g cm^{-3}.[9] In a second centrifugation run in methanol/bromoform mixture they measured a much higher density of 1.35 – 1.42 g cm^{-3}.[9] Comparing the sedimentation coefficient of the PNIPAM microgels measured in AUC to

their size measured in DLS led to a significantly lower density of 1.01 - 1.06 g cm^{-3}. The differences in the experimental measurements demonstrate that the density measurement methods, which are well established for solid particles, have to be used with care for significantly swollen microgels. In particular, discrepancies might originate from the interaction of the microgel network with the different solvents. The solvent may partially replace hydrogen-bound water by solvent molecules,[13,14] as well as replace non-hydrogen-bound water in the microgel network, thus leading to a change in microgel density. This preferential absorption can severely falsify the densities retrieved from the AUC studies.

Due to these critical aspects when exposing highly solvated microgels to a density gradient or solvent mixture, we focus in our study on a different strategy. Using AUC sedimentation velocity experiments, we determined the sedimentation coefficients for the microgels. Using further the diffusion coefficient measured by DLS and the partial specific volume determined by density measurements, the anhydrous mass of the microgels was calculated. Notably, this mass still contains contributions from hydrogen-bond water. As mentioned before, the reason is that the mass of the microgel powder determined prior to preparing the concentrations for the density measurements directly defines which partial specific volume is calculated and which mass is retrieved from the AUC experiment.[15] Hydrogen-bound water could not be removed prior to weighting the powder for the density measurements.

We characterized the density of PNIPAM microgels in aqueous dispersions as well as the polymer content within the microgel in the swollen and the collapsed state as a function of the crosslinking density. We synthesized a set of PNIPAM microgels with similar diameter in the collapsed state but different crosslinking densities.[1] The concentration of the crosslinker (BIS) was varied from 1 to 10 mol-%. The crosslinking density influences the swelling behaviour the microgels, with an increase in hydrodynamic diameter for softer, less crosslinked microgels below the volume phase transition temperature (Figure S3a). We further used AUC to measure the sedimentation coefficient of the microgels in the swollen state (20 °C, Figure S3b, full line) and in the collapsed state (40 °C, Figure S3b, dotted line). Since the viscosity of water decreases with increasing temperature and thus affects the sedimentation coefficient (Equation 4), we corrected the sedimentation coefficient for water at 20 °C. We observe two clear trends. First, microgels in the collapsed state sediment faster compared to their swollen counterparts. Second, microgels sediment faster with increasing crosslinking densities. Using

Stokes' law (Equation 4) and the hydrodynamic volume measured by DLS (Figure S3a), we calculate the effective density of the microgels in the swollen (Figure S3c, full square) and collapsed (Figure S3c, hollow square) state. In the swollen state, we determine effective densities between 1.004 g cm^{-3} and 1.021 g cm^{-3}. We notice a clear trend to higher microgel densities with increasing crosslinking densities caused by the lower swelling and thus lower bulk water content. In the collapsed state at 40 °C, the density of the microgels is significantly higher compared to the swollen state and ranges from 1.064 g cm^{-3} to 1.071 g cm^{-3} with a clear trend of increasing density with increasing crosslinking density. However, the trend to higher densities with increasing crosslinking densities is significantly lower compared to the swollen state and can be the result from a different density of the monomer PNIPAM and the crosslinker BIS. Most notably, the results are in agreement with previous measurements on similar microgels using AUC.[9]

We further measured the density of microgel suspensions with known concentrations to derive the partial specific volume. Using Equation 3, the anhydrous mass of the PNIPAM microgels can be calculated. Noteworthily, this mass still includes contributions from hydrogen-bound water, which could not be removed when drying the microgels. Dividing the effective microgel mass measured by AUC and DLS by the anhydrous mass of the polymer, we obtain the polymer mass fraction (Figure S3d) including hydrogen-bound water. At 20 °C, we determine a polymer weight fraction between 4 wt-% and 14 wt-%, which increases with increasing crosslinking densities due to the reduced swelling. Assuming that the polymer mass and the amount of hydrogen-bound water to the microgel does not change with temperature, we calculate the polymer mass fraction in the collapsed state at 40 °C, which is between 50 wt-% and 60 wt-%. These results confirm previous calculations of the polymer density using static and dynamic light scattering.[16,17] Importantly, with our technique the mass fraction was determined, while using static light scattering the volume fraction was calculated. As PNIPAM has a higher density compared to water, the volume fractions should be lower compared to the mass fraction. Furthermore, it was assumed in our calculations that the PNIPAM mass does not change with temperature as partial specific volumes could not be measured with satisfactory reproducibility at 40 °C, most presumably due to outgassing of the solvent. However, during the phase transition at 32 °C ~3.5 hydrogen-bond water molecules are released,[18] leading to a lower polymer mass. Our calculations thus slightly overestimate

the polymer fraction. The decrease in polymer content with increasing crosslinking density may be explained by the additional geometrical restrictions due to the crosslinking points, hindering dense packing during the phase transition of the PNIPAM microgel to a collapsed state. All measured and calculated values related to the density and non-bound water content are summarized in Table 1.

Table 1: Experimental measurements for the calculation of the microgel density and polymer content.

Density solvent (20 °C)	kg/m³	998.244
Density solvent (40 °C)	kg/m³	992.193
Viscosity solvent (20 °C)	Pa*s	1.002E-03
Viscosity solvent (40 °C)	Pa*s	6.533E-04

Crosslinking density	mol-%	1	2.5	5	10
vbar (20 °C)	m^3/kg	8.657E-04	8.635E-04	8.546E-04	8.365E-04
x_H (20 °C)	nm	656.0	612.3	523.9	472.7
x_H (40 °C)	nm	267.5	273.3	285.9	292.8
S (20 °C)	S	1381	1699	2178	2843
S (40 °C)	S	4398	4830	5452	6088
ρ_{eff} (20 °C)	kg/m^3	1004.0	1006.4	1012.5	1021.3
ρ_{eff} (40 °C)	kg/m^3	1065.3	1066.2	1071.1	1071.7
m_{eff} (20 °C)	kg	1.48E-16	1.21E-16	7.63E-17	5.62E-17
m_{eff} (40 °C)	kg	1.05E-17	1.19E-17	1.30E-17	1.52E-17
m_{anhyd}(20 °C)	kg	6.30E-18	7.11E-18	7.34E-18	7.68E-18
Swelling	-	14.1	10.2	5.9	3.7
Polymer content (20 °C)	wt-%	4.2	5.9	9.6	13.7
Polymer content (40 °C)	wt-%	60.0	60.0	56.5	50.7

Supplementary Figures:

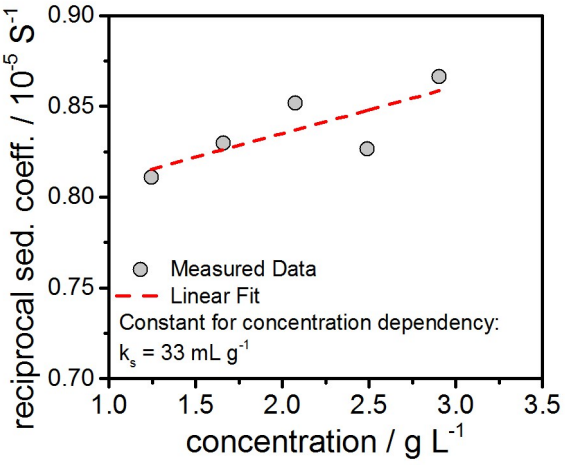

Supplementary Figure S1: Reciprocal sedimentation coefficient as a function of silica particle concentration. A moderate linear scaling coefficient of 33 mL g^{-1} was found for the friction factor. The silica nanoparticle concentration was kept constant for all experiments in order to minimize effects of hydrodynamic non-ideality.

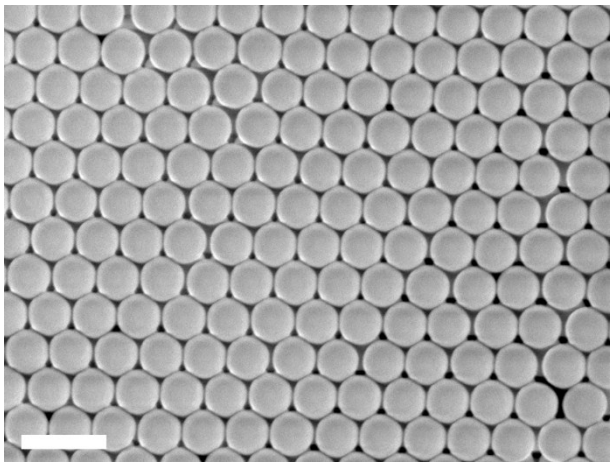

Supplementary Figure S2: SEM image of the synthesized Stöber particles. Scale bar: 1 µm

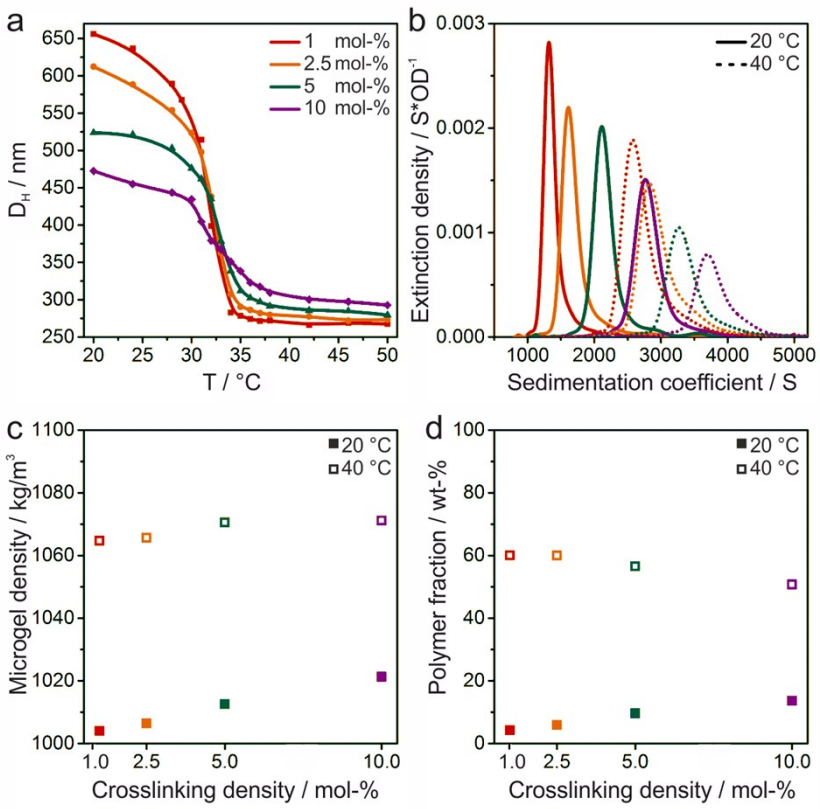

Supplementary Figure S3: Characterization of physicochemical properties of PNIPAM microgels with different crosslinking densities (1 mol-% (red), 2.5 mol-% (orange), 5 mol-% (green), 10 mol-% (purple)). a) Temperature-dependent hydrodynamic diameter measured by dynamic light scattering (DLS). b) Microgel sedimentation coefficient measured by analytical ultracentrifugation (AUC) below and above the volume phase transition at 20 °C (full line) and at 40 °C (dotted line). c) Microgel density calculated from hydrodynamic diameter and sedimentation coefficient as a function of crosslinking density at 20 °C (full) and at 40 °C (hollow). d) Microgel polymer weight fraction determined by the ratio of the microgel mass measured by AUC by the mass of the polymer obtained by Equation 3, we obtain the polymer mass fraction at 20 °C (full) and at 40 °C (hollow).

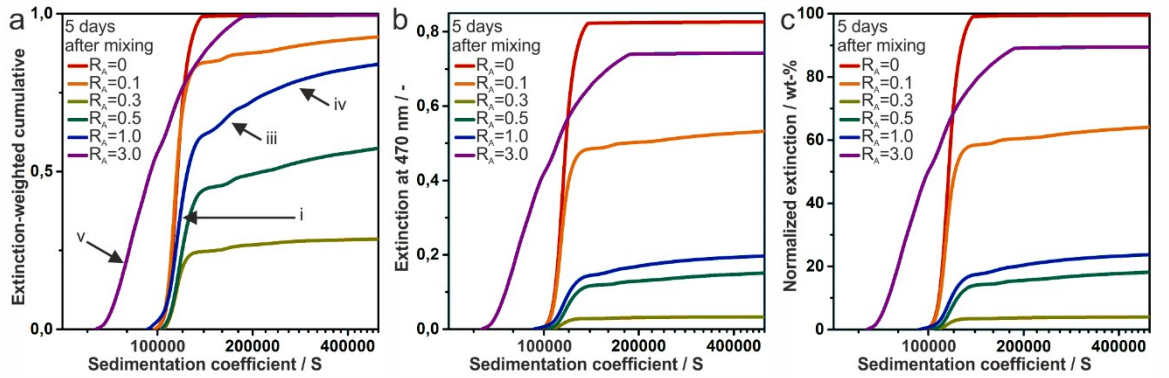

Supplementary Figure S4: Heteroaggregation of silica particles and smaller PNIPAM microgels at 20 °C characterized by AUC five days after mixing. a) Cumulative sedimentation coefficient distributions. b) Extinction at 470 nm as a function of the sedimentation coefficient distribution. c) Cumulative sedimentation coefficient distributions normalized to the extinction of pure silica at 470 nm where we observe a surface ratio-dependent R_A aggregation peaking for R_A = 0.3. Dimers (two particles bridged by one microgel) (iii) as well as larger aggregates (iv) can be identified in the sedimentation coefficient distribution. An excess of microgels is needed in order to stabilize the silica particles against aggregation (v).

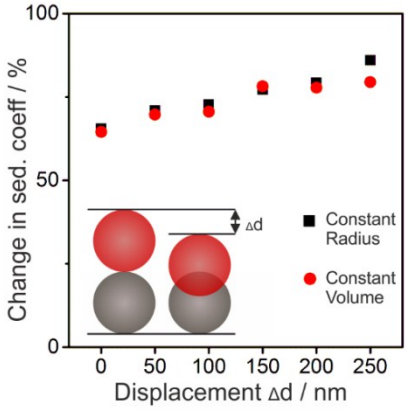

Supplementary Figure S5: Calculated shift in sedimentation coefficient as a function of microgel/particle overlap Δd, where the microgel radius (black) or the microgel volume was kept constant (red). The shape of the heteroaggregate influences the shift in sedimentation coefficient. With increasing overlap, the shift in sedimentation coefficient decreases.

Cumulative fraction of the individual species from AC

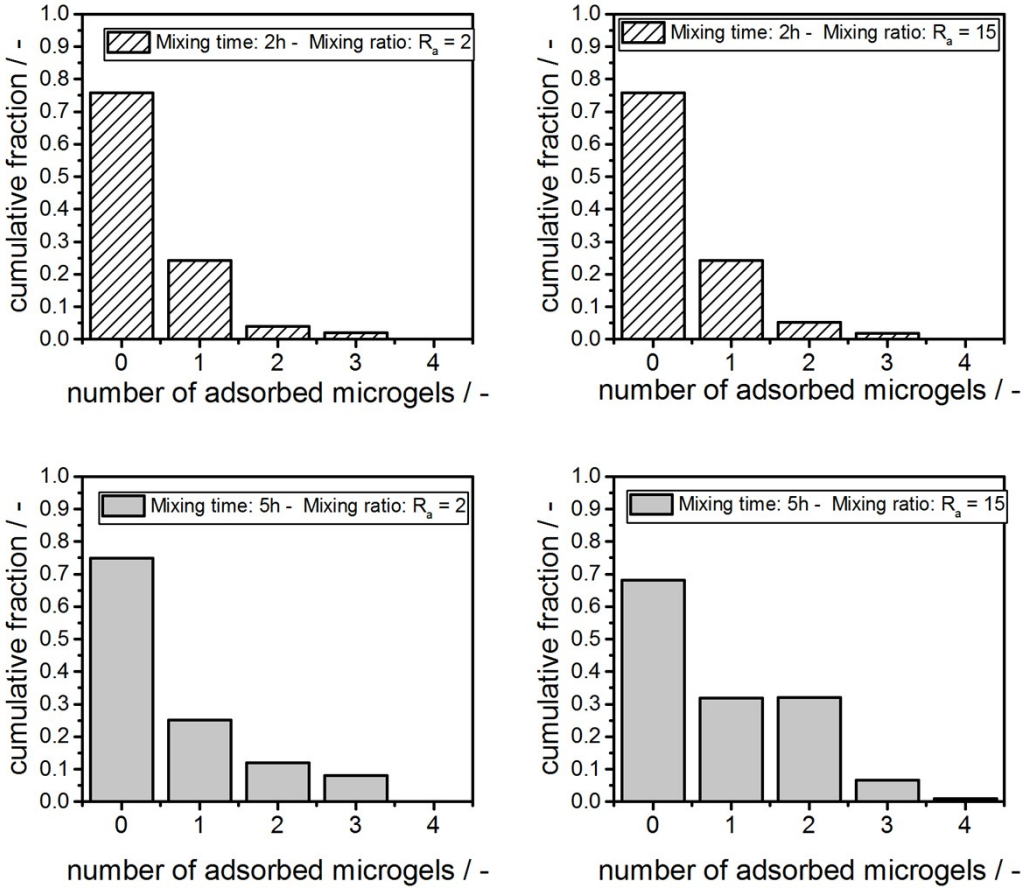

Figure S6: Cumulative fraction of individual species from Figure 1 b and 1 c in the main manuscript.

Brownian Dynamics algorithm.

The Brownian Dynamics simulations were performed according to the following algorithm. In the subsequent Figure, an arbitrarily shape object Ω is enclosed by an imaginary sphere with radius b. From the surface of the sphere, Brownian particles are launched from an initial position r=b. This motion of the particles is modelled according to:[19]

$$r = r_0 + \sqrt{2D\Delta t} \tag{S2}$$

Where D is the diffusion coefficient of the particle and Δt a certain time step. The motion of each particle is then tracked until it either hits the object Ω or crosses the starting surface at r=b. This particle will escape to infinity with a certain probability, which is given below, or return to the starting surface at r=b.

$$P_{esc} = 1 - \frac{b}{r_0} \tag{S3}$$

For illustrative purpose, the subsequent figure depicts one object used in our simulations, showing a core silica particle and two microgels, that are attached to its surface.

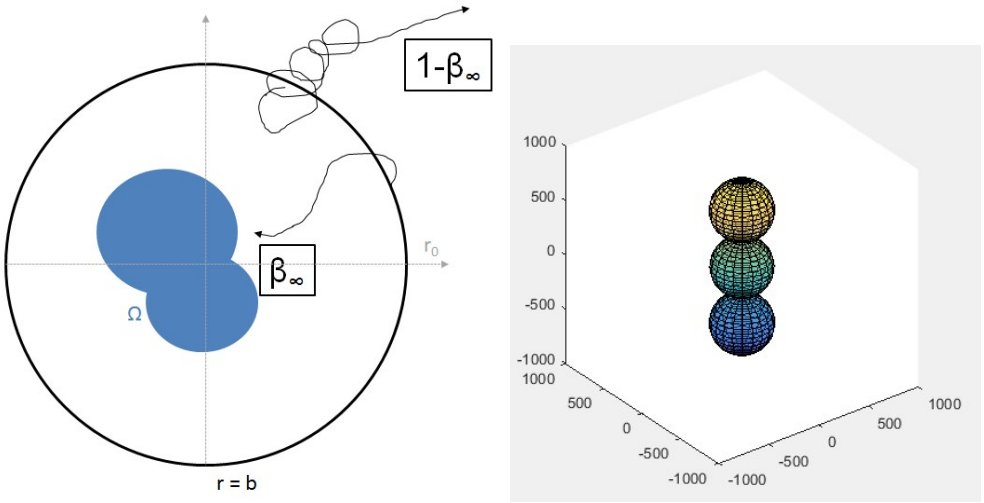

Figure S7: Left: Schematic representation of the Brownian Dynamics (BD) algorithm for the calculation of the hydrodynamic diameter xH. Adapted from Zhou et al..[20] Right: Representative object from our BD simulations. A core silica particle and two microgels, that are attached to its surface.

Zhou et al.[20] have shown how to correlate the hit fraction of an arbitrary shaped object β∞ of an infinite number of Brownian particles and the hydrodynamic diameter:

$$x_H = b\beta_\infty \quad \text{(S4)}$$

Moreover, the translational friction factor, which is later needed in order to calculate respective sedimentation coefficients, is related to the hydrodynamic diameter xH through the following Equation[21]:

$$f = 3\pi\eta x_H \quad \text{(S5)}$$

Calculation of volume overlap

Table S2: Calculation of occupied volume of the silica core particle as a function of the number of attached microgels. Values are calculated based on the model used throughout the BD simulations.

Number of attached microgels / #	1	2	3	4
Reduction in sedimentation velocity / -	See Figure 4	See Figure 4	See Figure 4	See Figure 4
Overlap Volume / 10^5 nm^3	142	284	426	568
Relative occupied volume / -	19.98%	39.96%	59.95%	79.93%

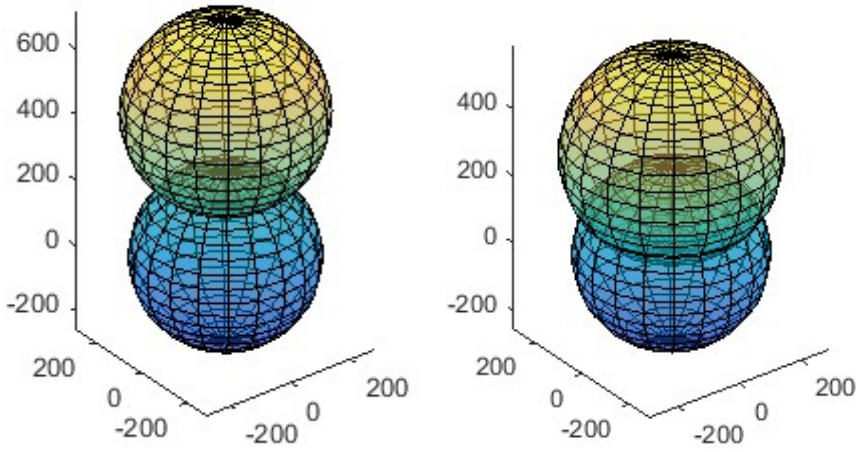

Figure S8: Illustration of the overlapping microgel and silica particle spheres.

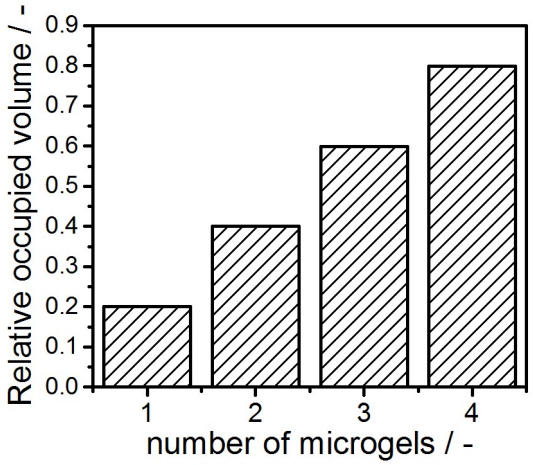

Figure S9: Relative occupied volume of the core silica particle as a function of the number of microgels.

References

1 M. Rey, X. Hou, J. S. J. Tang and N. Vogel, *Soft Matter*, 2017, **13**, 8717–8727.

2 X. Wu, R. H. Pelton, A. E. Hamielec, D. R. Woods and W. McPhee, *Colloid Polym. Sci.*, 1994, **272**, 467–477.

3 W. Stöber, A. Fink and E. Bohn, *J. Colloid Interface Sci.*, 1968, **26**, 62–69.

4 J. Walter and W. Peukert, *Nanoscale*, 2016, **8**, 7484–7495.

5 P. Schuck and P. Rossmanith, *Biopolymers*, 2000, **54**, 328–341.

6 M. Zanini, C.-P. Hsu, T. Magrini, E. Marini and L. Isa, *Colloids Surfaces A Physicochem. Eng. Asp.*, 2017, **532**, 116–124.

7 A. K. Lele, M. M. Hirve, M. V. Badiger and R. A. Mashelkar, *Macromolecules*, 1997, **30**, 157–159.

8 L.-C. Dong and A. S. Hoffman, *J. Control. Release*, 1990, **13**, 21–31.

9 K. Tauer, D. Gau, S. Schulze, A. Völkel and R. Dimova, *Colloid Polym. Sci.*, 2009, **287**, 299–312.

10 L. Zhang, E. S. Daniels, V. L. Dimonie and A. Klein, *J. ofAppliedPolymer Sci.*, 2010, **118**, 2502–2511.

11 J. Walter, *Multidimensional Characterization of Nanoparticles by Means of Analytical Ultracentrifugation*, Dr. Hut., 2017.

12 O. Kratky, H. Leopold and H. Stabinger, *Methods Enzymol.*, 1973, **27**, 98–10.

13 D. Mukherji, C. M. Marques and K. Kremer, *Nat. Commun.*, 2014, **5**, 1–6.

14 I. Anac, A. Aulasevich, M. J. N. Junk, P. Jakubowicz, R. F. Roskamp, B. Menges, U. Jonas and W. Knoll, *Macromol. Chem. Phys.*, 2010, **211**, 1018–1025.

15 R. Schuck, P., Zhao, H., Brautigam, C. A., & Ghirlando, *CRC Press*.

16 C. G. Lopez and W. Richtering, *Soft Matter*, 2017, **13**, 8271–8280.

17 I. Varga, T. Gilányi, R. Mészáros, G. Filipcsei and M. Zrínyi, *J. Phys. Chem. B*, 2001, **105**, 9071–9076.

18 K. Shiraga, H. Naito, T. Suzuki, N. Kondo and Y. Ogawa, *J. Phys. Chem. B*, 2015, **119**, 5576–5587.

19 D. L. Ermak and J. A. McCammon, *J. Chem. Phys.*, 1978, **69**, 1352–1360.

20 H. X. Zhou, A. Szabo, J. F. Douglas and J. B. Hubbard, *J. Chem. Phys.*, 1994, **100**, 3821–3826.

21 A. L. Kholodenko and J. F. Douglas, *Phys. Rev. E*, 1995, **51**, 1081–1090.